Promotional effect of ceria on the catalytic behaviour of new V2O5–WO3–TiO2 aerogel solids for the DeNOx process

Jihene Arfaoui, Abdelhamid Ghorbel, Carolina Petitto, Gérard Delahay

Promotional effect of ceria on the catalytic behaviour of new V_2O_5-WO_3-TiO_2 aerogel solids for the DeNOx process

Jihene Arfaoui[*a], Abdelhamid Ghorbel[a], Carolina Petitto[b], Gerard Delahay[b]

[a]Université Tunis El Manar, Laboratoire de Chimie des Matériaux et Catalyse, Département de Chimie, Faculté des Sciences de Tunis, Campus Universitaire Farhat Hached d'El Manar, 2092, Tunis, Tunisia.

[b]ICGM, Univ Montpellier, ENSCM (MACS), CNRS, Montpellier, France

* Corresponding author: E-mail address: jihene.arfaoui@fst.utm.tn; jihenar@yahoo.fr

Tel: +216 23020273, Fax: +216 71 875 008

Abstract

New cerium and/or tungsten modified V_2O_5-TiO_2 aerogel catalysts (V_2O_5-TiO_2,V_2O_5-WO_3-TiO_2, V_2O_5-CeO_2-TiO_2 and V_2O_5-WO_3-CeO_2-TiO_2) were successfully developed, by associating the sol gel procedure and supercritical drying approach. A combination of various analytical techniques, including XRD, N_2-Physisorption at 77 K, DRUV-Vis spectroscopy, NH_3-TPD and H_2-TPR, was used to characterize the obtained solids. Their catalytic performances were evaluated in the low temperature NO-SCR by NH_3. The results reveal that all the materials exhibit high cristallinity of TiO_2 anatase phase and developed mesoporous texture. The addition of tungsten (W) increases the surface acidity of V_2O_5-TiO_2 and thereby enhances its reactivity at high temperatures (> 420 °C). However, the addition of cerium (Ce) improves the redox properties of the latter catalyst and increases significantly its NO-SCR reactivity, especially at low temperatures. The NO-SCR activity increases over the aerogel systems, in the 200-400 °C temperature range, following this order: V_2O_5-WO_3-TiO_2 < V_2O_5-TiO_2 < V_2O_5-CeO_2-TiO_2 < V_2O_5-WO_3-CeO_2-TiO_2. The new V_2O_5-WO_3-CeO_2-TiO_2 system was found to be the most active catalyst for converting NO into N_2 (with 60 % and 90 % NO conversions at 250 °C and between 320 and 420 °C, respectively). The highest SCR activity of this new aerogel solid if compared to the other samples was essentially correlated with a good reactivity of its acidic and redox sites which in turn was related to the existence of

strong interactions between cerium and the other active elements (mostly Ce↔ V and Ce ↔ W).

Key words: Environmental remediation, DeNOx process, Transition metals, Rare earths, New aerogel solids, Modified V_2O_5-TiO_2

1. Introduction

Simple/complexed oxides are a wide class of materials, with diverse crystal structures, which can be synthezised via different methods and are characterized by amazingly diverse properties (acidic, basic, redox, electric, dielectric, optical, magnetic, photocatalytic, catalytic, electrochemical, ferroelectric, piezoelectric, semiconductivity, ionic conductivity …) which make them quite useful in a large range of applications including electro-optical, electro-mechanical, electronics, energy storage, drug delivery, magnetic resonance imaging, biosensors and catalysis [1-14]. Recently, transition metal oxides have demonstrated high catalytic performance in the selective catalytic reduction (SCR) of nitrogen oxides (NO_x) by ammonia (NH_3) [15].

Nitrogen oxides (NOx, x = 1, 2), discharged from power plants, waste incinerators, industrial boilers, engines and automobiles, can cause adverse effects to the human health (bronchitis, pneumonia…) and contribute to a series of environmental issues (photochemical smog, acid rain, ozone decline in middle to high latitudes from spring to fall, biological death of lakes and rivers…) [16,17]. Many control technologies have been developed in order to reduce NOx emissions. Among them, the NH_3-SCR has been proved to be one of the most successful methods for the purification of NOx from stationary sources and diesel vehicles [18-20]. A variety of NH_3-SCR catalysts, including noble metals, zeolites, carbon-based catalysts and transition metal oxides have been explored [21-23]. Especially, V_2O_5/TiO_2 systems, promoted by WO_3 or MoO_3, have been extensively used in the industry and demonstrated an excellent NOx removal efficiency in the 300-400 °C temperature range [24-29]. For such catalysts: TiO_2 is employed as a carrier because of its high surface area and porosity which are beneficial for the catalytic reactions and reactants adsorption.V_2O_5 is the main active substance, which generates active redox sites and exhibits strong catalytic activity and stability, while WO_3 or MoO_3 act as ‘chemical’ and ‘structural’ promoter by enlarging the

temperature window of the SCR reaction, limiting the oxidation of SO_2 and improving the mechanical strength of catalysts [30].

Generally, the high activity and stability of supported metal oxide catalysts depend on the active sites dispersion and metal-support interactions. In this respect, the preparation method is a vital factor to determine the phase composition, configuration and dispersion of the active components. Therefore, it is crucial to find the appropriate preparation method to optimize the SCR performances of catalysts [31]. According to the literature reports, the main synthesis methods of V_2O_5-TiO_2-based SCR catalysts are (wet, dry, incipient wetness and ultrasound- assisted)-impregnation [27,32-35], co-precipitation [34] and deposition-precipitation [35-37]. Pang et al. [35] showed that the ultrasound- assisted impregnation method produced a stronger interaction between the vanadium species and WTi support, which stabilized these species in the reduced state and leads to more active VWTi SCR catalyst compared to the same one obtained via the conventional impregnation method. On the other hand, He et al. [34] concluded that the SCR activity is always greater for the VWTi co-precipitated catalysts compared to the impregnated VWTi ones for the same catalyst composition and surface area.

In recent years, cerium has been extensively studied as an accessory element for NH_3-SCR catalysts because of its high oxygen storage capacity (OSC) and remarkable redox properties [38-40]. CeO_2 is also considered as the active component in the SCR reaction due to its ability to enhance the oxidation of NO to NO_2 [41]. In addition, oxygen vacancies exist on the CeO_2 surface which facilitates the adsorption and activation of NO and NH_3, and subsequently increases the NH_3-SCR activity [42]. Chen et al. [42] investigated the effect of the additive Ce on V_2O_5-WO_3/TiO_2 system for the selective catalytic reduction (SCR) of NOx with NH_3. Their results showed that adding Ce could enhance the NOx adsorption and then accelerate the SCR reaction due to the synergetic interaction between the Ce and V, W

species. Cheng et al. [43] demonstrated that the SCR activity of V_2O_5-WO_3/TiO_2, elaborated by the homogeneous precipitation method, was greatly enhanced by Ce doping (molar ratio of Ce/Ti = 1/10) in the TiO_2 support. However, Hu et al. [44], reported that CeO_2-V_2O_5-WO_3/TiO_2 catalysts, obtained via the impregnation method, exhibited a higher NH_3-SCR activity and better Na resistance than the V_2O_5-WO_3/TiO_2 catalyst.

Based on the above discussion, and taking into account *(i)* the advantages of using the sol gel method for the preparation of highly active aerogel catalysts for the DeNOx process ([45-48] and *(ii)* that until now, any research work has not been devoted to the investigation of VWTi and VWCeTi aerogel solids in the NH_3-SCR reaction, it appeared interesting to develop in this work a new V_2O_5-WO_3-TiO_2 and V_2O_5-WO_3-CeO_2-TiO_2 aerogel catalysts, containing V and W amounts representative of V_2O_5-WO_3/TiO_2 commercial SCR catalyst (2% wt. V_2O_5 and 10 % wt. WO_3), for the selective catalytic reduction of NO by NH_3 from diesel engine exhaust. It is worth mentioning that Ce and W species were added in order to improve the redox and acidic performances to V_2O_5-TiO_2 system, respectively. In fact, it is established that both acidic and redox properties of catalyst are the key factors which govern its SCR activity [49]. It was revealed that the surface acidity plays an important role in the adsorption and activation of ammonia, especially at high temperature. However, the reactivity of catalyst is controlled, at low temperature, by its redox behaviour [49].

2. Material and methods

2. 1. Aerogel catalysts preparation

It is well known that, several advantages distinguish the sol-gel procedure including a simple technology, low processing temperature and flexible control of the structure and size of final products via many operating parameters [50,51]. Therefore, this method was adopted in this work for the elaboration of aerogel samples (TiO_2, V_2O_5-TiO_2, V_2O_5-WO_3-TiO_2, V_2O_5-CeO_2-TiO_2 and V_2O_5-WO_3-CeO_2-TiO_2) according to the same procedure described in our

previous works [45,46]. Vanadyl acetylacetonate ($V(C_5H_7O_2)_2$, Fluka, 95%), ammonium metatungustate hydrate ($(NH_4)_6H_2W_{12}O_{24}.xH_2O$, Sigma Aldrich, > 99.9%) and cerium nitrate ($Ce(NO_3)_3.6H_2O$, Aldrich) were used as V, W and Ce precursors. Theoretical loading of V_2O_5, WO_3 and CeO_2 were fixed to 2, 10 and 10 % wt., respectively. All the aerogel mixed oxides were calcined at 500 °C for 3 h under O_2 flow (30 mL.min^{-1}).

2. 2. Aerogel catalysts characterization

The powder X ray diffraction (XRD) patterns were registered, between 2 and 80 °, by means of a Brüker AXS D8 diffractometer, using CuKα radiation (λ = 1.5406 Å). The Scherrer formula ($D = 0.89 (\lambda / \beta \cos\theta)$) [43], applied to the most intense peak of TiO_2 anatase phase (~2θ = 25 °), was used for the calculation of the crystallites size (D) of samples. λ is the wavelength of XR radiation, β is the corrected peak width at half-maximum intensity (FWHM in radians), and θ is the peak position of the main reflection.

The textural properties of solids (specific surface area (S_{BET}), total pore volume (V_{PT}) and pore size diameter (Φpore)) were determined by N_2 adsorption-desorption at 77 K with a Micromeritics ASAP 2020 equipment. Prior to adsorption measurement, the sample was degassed in an evacuation chamber at 200 °C.

The UV-vis diffuse reflectance absorption spectra of powder aerogels were collected at room temperature on a PerkinElmer spectrophotometer type lambda 45 equipped with an integrating sphere type RSA-PE-20. The scanning range was between 200 nm and 900 nm.

The NH_3 temperature-programmed desorption (NH_3-TPD) analyses were performed using an AUTOCHEM 2920 (Micromeritics) equipped with a TCD detector. A 0.05 g of each catalyst was loaded in the reactor and was pretreated in air flow (30 mL min^{-1}) at 500 °C (ramp 10 °C min^{-1}) for 30 min, and then cooled to 100 °C in the same stream. Afterward, the pretreated sample was exposed to NH_3 (5 vol% NH_3 in He, flow rate = 30 mL min^{-1}) for 45 min. The physisorbed NH_3 was removed by flushing the catalyst with He at a flow rate of 30

mL min^{-1} for 2 h before starting the TPD experiment. The NH_3-TPD curves were recorded by heating the samples in He (30 mL min^{-1}) from 100 to 600 °C at a heating rate of of 10 °C min^{-1}.

The H_2 temperature-programmed reduction (H_2-TPR) experiments were carried out in an AUTOCHEM 2910 (Micromeritics) using 0.05 g of catalyst. Prior to the analysis, the sample was pretreated at 500 °C with 5 vol % O_2 in He (30 mL min^{-1}) for 30 min (ramp 10 °C min^{-1}). The TPR experiments were realized using a stream of 5 vol % H_2 in Ar (30 mL min^{-1}) from 50 to 800 or 900 °C at a heating rate of 10 °C min^{-1}. The hydrogen consumption was measured by a thermal conductivity detector.

2. 3. Catalytic performance test

The selective Catalytic Reduction (SCR) tests were done in a fixed-bed quartz flow reactor, operating at atmospheric pressure, using the following reaction conditions: 400 ppm NO, 400 ppm NH_3, 8 % O_2 in He and 100 mL min^{-1} total flow rate yielding a gas hourly space velocity (GHSV) of 120,000 h^{-1}. Before measurements, the catalyst (0.05 g) was activated in situ at 200 °C for 30 min under O_2/He (20/80, v/v) flow then cooled to 100 °C. Afterward, the NO conversion curves were recorded between 100 and 500 °C with the heating rate of 6 °C min^{-1}. The reactants and products gases were continuously analyzed by an online Pfeiffer Omnistar quadruple mass gas spectrometer equipped with Channeltron and Faraday detectors (0-200 amu).

3. Results and discussion

3. 1. Characterization of aerogel catalysts

The structural properties of samples were examined by XRD, the results are given in Fig 1 and Table 1. As shown in Fig 1, the dominant phase in all the XRD patterns is TiO_2 anatase which is identified by its characteristic peaks located at $2\theta \approx 25.3°$ (hkl:101); 36.9°(103); 37.8° (004); 38.6° (112); 48.2° (200); 53.9° (105); 55.2° (211); 62.7° (204); 69.0°

(116); 70.4° (220) and 75.2° (215) [ICSD 01-083-2243]. Additional minor peak is observed at 2θ = 27.2° (110) in the diffractograms of V_2O_5-TiO_2 and V_2O_5-WO_3-CeO_2-TiO_2 catalysts and is attributed to a trace amount of theTiO_2 rutile phase [ICSD 01-076- 1941]. Noting that a low amount of cubic CeO_2 seems to be formed at the surface of V_2O_5-WO_3-CeO_2-TiO_2, since ~~a~~ new peaks of low intensity are detected at 2θ ≈ 28.5° (hkl: 111) and 32.9° (200) [ICSD 00-034-0394] on the diffractogram of the previous cited sample. It is worth mentioning that the absence of reflections related to crystallines phases V_2O_5 (major one at 2θ = 20.2° (001) [ICSD 01-089-2482]) and WO_3 (major one at 2θ ≈ 23,7° (hkl: 110) [ICSD 01-089-8053]) for all the catalysts and the presence of a low quantity of cubic CeO_2 in the case of V_2O_5-WO_3-CeO_2-TiO_2 only indicate, in line with the results already obtained by Hu et al. [44], for comparable systems, that V, W and Ce species are well dispersed and exist in the form of monolayer species at the surface of TiO_2 carrier. Based on the above XRD results and taking into account the values of the crystallites size of powder aerogels (ranging between ~ 9 and 29 nm, Table 1), it can be concluded that all the obtained catalysts are well structured materials with a nanometer size of grain. It should be mentioned the addition of vanadium, tungsten and cerium contributes to the growth of the TiO_2 cristallites size. This may be due to the agglomeration of the metal clusters to form larger particle size [52]. Furthermore, the formation of trace amount of the TiO_2 rutile phase, in the case of V_2O_5-TiO_2 and V_2O_5-WO_3-CeO_2-TiO_2 catalysts, contributes also to the increase of the cristallites size of titania carrier [53].

Table 1. XRD phases and TiO_2 crystallites size of aerogel catalysts.

Aerogel mixed oxides	XRD phases	FWHM (°)	TiO_2 crystallites size D (nm)
TiO_2	A	0.892	8.6
V_2O_5-TiO_2	A + R (t)	0.626	12.4
V_2O_5-CeO_2-TiO_2	A	0.761	10.2
V_2O_5-WO_3-TiO_2	A	0.808	9.5
V_2O_5-CeO_2-WO_3-TiO_2	A + R (t) + CeO_2 (t)	0.266	28.8

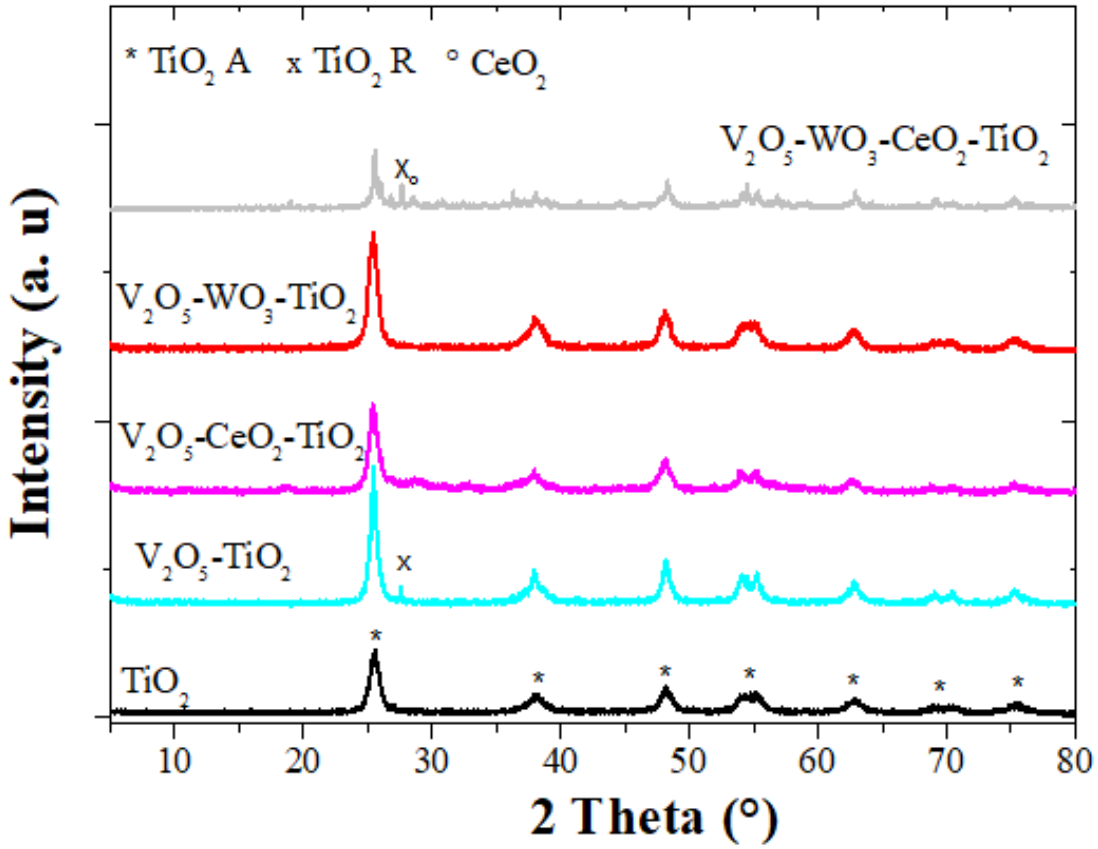

Figure 1. Powder XRD patterns of aerogel catalysts.

The textural properties of samples are given in Table 2. It is clearly seen that all the aerogel oxides, except for the V_2O_5-WO_3-CeO_2-TiO_2 solid, display a developped texture with a high surface area ($82 \leq S_{BET} \leq 128$ m^2/g) and total pore volume ($0.33 \leq V_{PT} \leq 0.41$). The lowest values of the S_{BET} and V_{PT}, obtained in the case of V_2O_5-WO_3-CeO_2-TiO_2 catalyst,

could reveal the blockage of some pores of TiO_2 carrier by V, W and/or Ce supported species. This is consistent with the result already obtained by Hu et al. [44] demonstrating that the BET surface area and total pore volume of VWTi catalysts tend to decrease after doping CeO_2, and this tendency is more obvious with the higher amount of CeO_2. The authors suggested that the highly dispersed CeO_2 blocks the micropores of catalysts.

Table 2. Textural properties of aerogel catalysts.

Aerogel mixed oxide	BET surface area (m^2/g)	Total pore volume (cm^3/g)	Average Pore diameter (Φ_{pore}, Å)
TiO_2	122	0.33	79
V_2O_5-TiO_2	101	0.37	117
V_2O_5-CeO_2-TiO_2	82	0.33	133
V_2O_5-WO_3-TiO_2	128	0.41	111
V_2O_5-CeO_2-WO_3-TiO_2	43	0.21	158

The N_2 adsorption-desorption isotherms at 77 K and pores size distribution curves of samples are displayed in Fig. 2. It is clearly seen that, all the catalysts are characterized by a type IV isotherm, typical of mesoporous materials according to the IUPAC classification [54], and unimodal porous distribution with diverse types of hysteresis loops. So, the H1 type of hysteresis, revealing the presence of cylindrical mesoporous channels [55], is obtained in the case of V_2O_5-TiO_2, V_2O_5-CeO_2-TiO_2 and V_2O_5-WO_3-CeO_2-TiO_2 samples. However, the hysteresis loop of H2 type is found for the TiO_2 and V_2O_5-WO_3-TiO_2 solids and it indicates the presence of ink-bottle pores in their mesoporous texture [56].

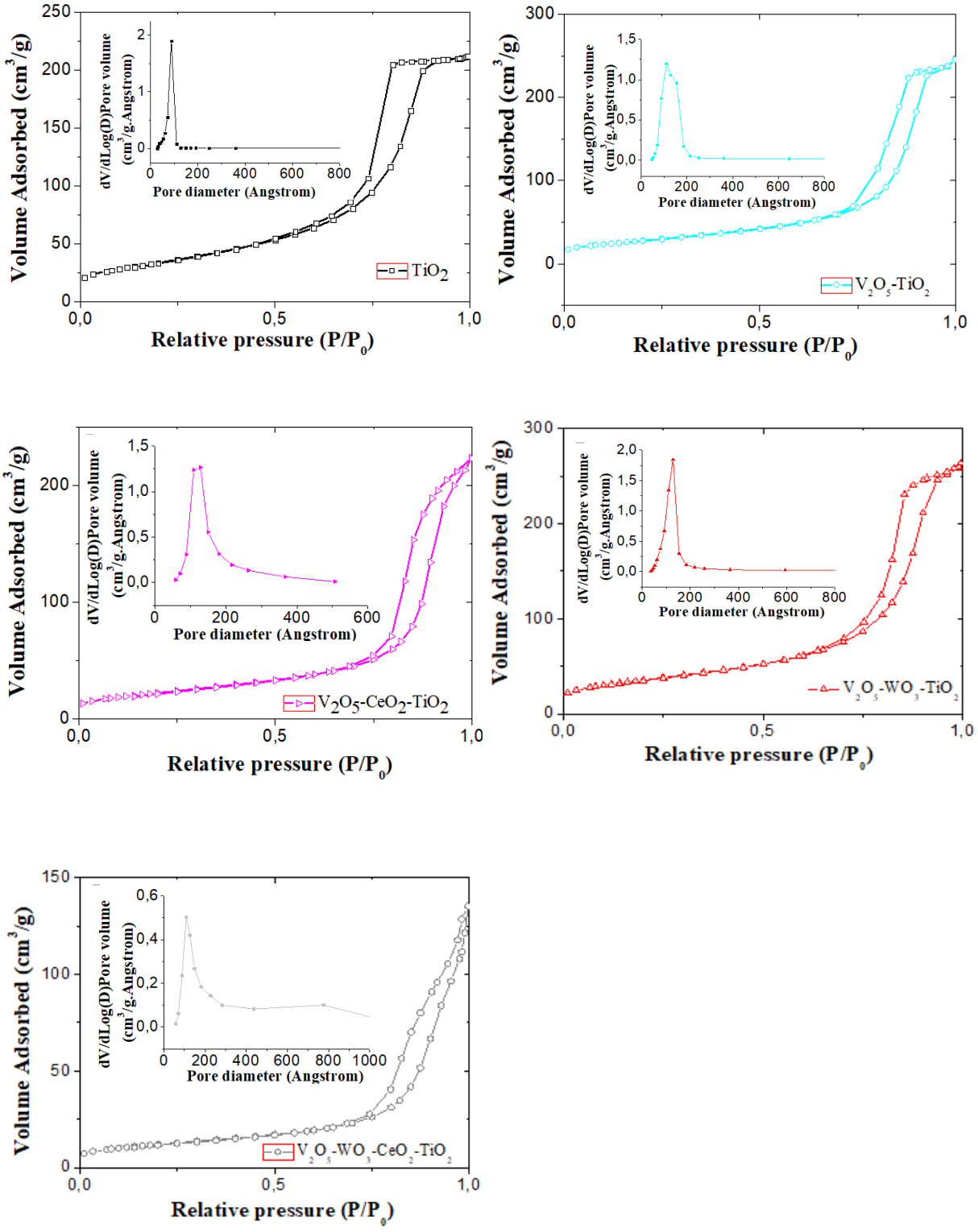

Figure 2. N_2 Adsorption-desorption isotherms and pore size distribution curves of aerogel catalysts.

Fig. 3 shows the UV-Vis diffuse reflectance spectra of different catalysts. According to the literature reports [45,57], the typical absorption bands of TiO_2 are situated between 200 and 400 nm, which are attributed to the $O^{2-} \rightarrow Ti^{4+}$ charge transfer corresponding to the excitation of electrons from the O2p valence band to the Ti3d conduction band. Additional bands with different intensities are observed in the 350-400 nm range for the catalysts containing vanadium and/or cerium which could be assigned to $O^{2-} \rightarrow V^{5+}$ charge transfer (CT) transitions in various VOx surface species [57,58] and /or $O^{2-} \rightarrow Ce^{4+}$ CT transitions of hexacoordinated cerium species [45,59]. It is worthy to note that, tungsten, vanadium and cerium species can display absorption bands corresponding to $O^{2-} \rightarrow M^{n+}$ CT transitions (M = W, V or Ce) in the same region than those of TiO_2 support as it was indicated in table 3. It should be noted also that the weak bands located at around 520 nm and 665 nm on the UV spectra of all the catalysts can be ascribed to a low amount of crystalline V_2O_5, probably too small to be detected by XRD technique, and to V^{4+} d–d transitions, respectively [60]. Nevertheless, no band related to the crystalline phase of WO_3 (usually at 430-450 nm [61]) is detected in the UV spectra of aerogels containing tungsten. Based on the obtained UV-vis results, it can be suggested the presence of a diversity of highly dispersed cerium, vanadium and tungsten species at the TiO_2 surface.

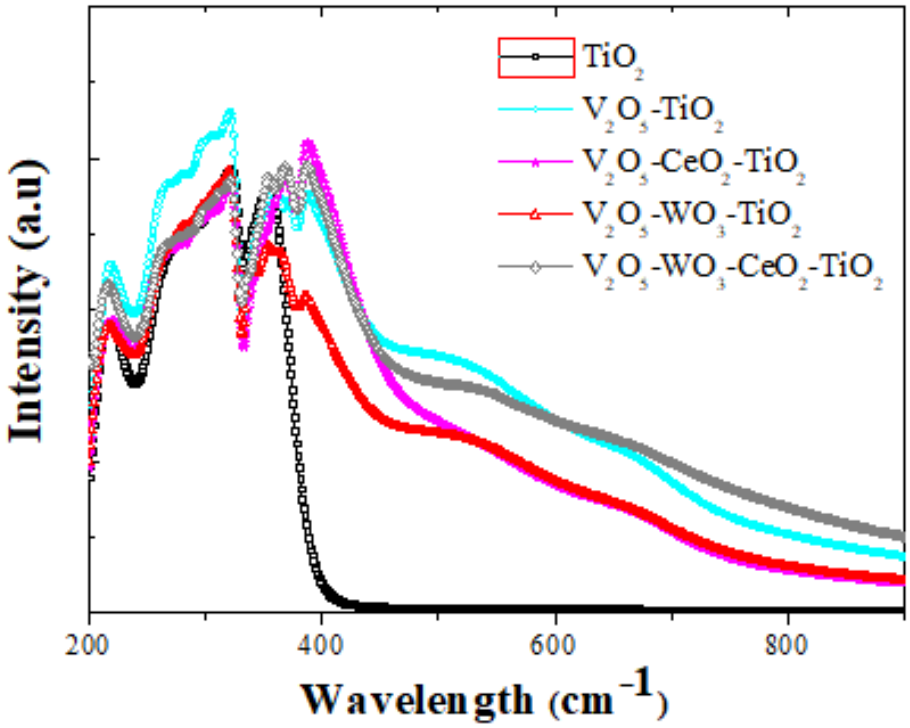

Figure 3. DRUV-Vis spectra of aerogel catalysts.

Table 3. UV-vis diffuse reflectance band positions and assignments found in the literature for M species (M = V, Ce and W).

M	DRUV-vis band Position: λ (nm)	Type of transition	Assignments	Ref.
V	240-280	$O^{2-} \rightarrow V^{4+}$ LMCT	Monomeric tetrahedral V^{4+} species	[46,62]
	280-340	$O^{2-} \rightarrow V^{5+}$ LMCT	Monomeric tetrahedral V^{5+} species	[46,62]
Ce	220-250	$O^{2-} \rightarrow Ce^{3+}$ LMCT	tetracoordinated Ce^{3+}	[63,64]
	280-300	$O^{2-} \rightarrow Ce^{4+}$ LMCT	tetracoordinated Ce^{4+}	[63,64]
W	220-240	$O^{2-} \rightarrow W^{6+}$ LMCT	Isolated tetrahedral W^{6+}	[55]
	320-340	$O^{2-} \rightarrow W^{6+}$ LMCT	Polymeric octahedral W^{6+}	[55]

Acid sites are the adsorption and activation sites for ammonia during the NH_3-SCR reaction. Therefore, the surface acidity of samples was examined by NH_3-TPD technique and the results are depicted in Fig. 4. As it can be seen the strength and the number of acid sites are clearly affected by the type of the elements added to titania oxide. So, the highest total acidity is obtained in the case of V_2O_5-WO_3-TiO_2 catalyst which displays the most intense and large NH_3 desorption peaks between 100 and 550 °C corresponding to the ammonia desorbed from weak, medium and strong acid sites [47,65]. As shown also in Fig. 4, a higher number of acid sites, related to NH_3 desorption in the100-400 °C temperature range, exist at the surface of V_2O_5-CeO_2-TiO_2 compared to that of V_2O_5-TiO_2. This result reveals, in agreement with many previous reports [4,66-69], that cerium and, particularly, tungsten species contribute to the creation of new and diverse acid sites at the surface of V_2O_5-TiO_2 catalyst. It seems that these new acid sites are generated by the presence of W and Ce species and through the interactions developed between them and with Ti and/or V elements. Noting that the lowest acidity is registered in the case of V_2O_5-WO_3-CeO_2-TiO_2 solid suggesting that the simultaneous presence of V, W and Ce species had a negative effect on the surface acidity of this aerogel catalyst. This is probably due to the existence of concurrent interactions between V, W and Ce species or between these supported species and the TiO_2 support which influence the surface acidity of solid. Similar result, revealing a visible decrease of the surface acidity of the zirconia after adding cerium, molybdenum and tungsten species, was reported in our previous work and was related to the existence of diverse interactions between the support and the supported active species which cover or change the nature of acidic sites at the ZrO_2 surface [47].

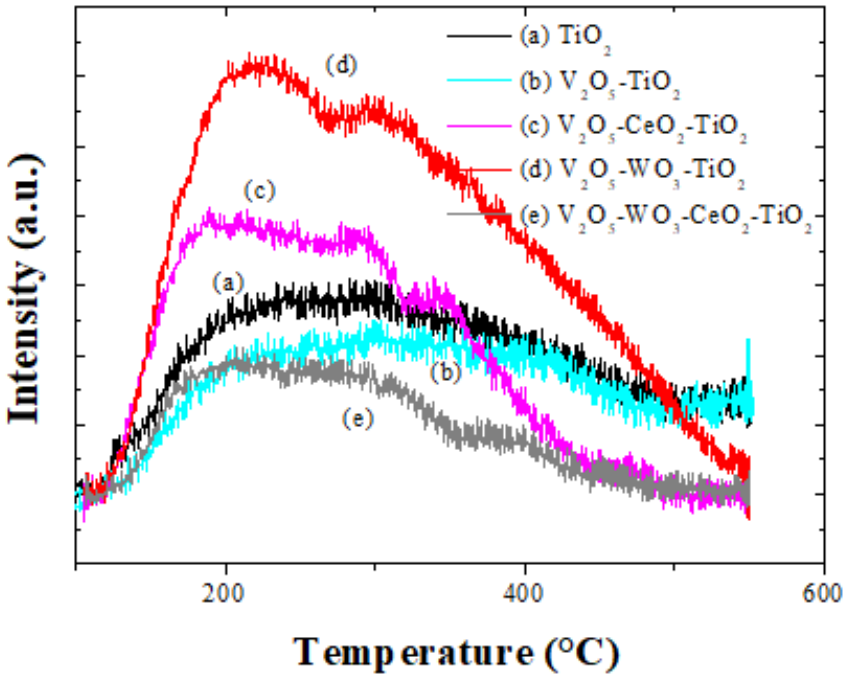

Figure 4. NH_3-TPD profiles of aerogel catalysts.

In addition to the surface acidity, the redox behaviour of catalyst had a great influence on the SCR reaction. Herein, the H_2-TPR analyses were done to examine the redox properties of aerogel solids and the obtained results are shown in Fig. 5. As it can be noticed, two unresolved peaks, maximizing at 430 and 500 °C, are observed for the binary V_2O_5-TiO_2 and can be ascribed to the reduction of highly dispersed VOx species [42,46]. When W or Ce species were introduced into V_2O_5-TiO_2 system, a new H_2 consumption peaks are appeared at different temperatures indicating the creation of new and various redox sites at the catalysts surface. Hence, the well resolved peak beginning at ~ 370 °C, with a maximum at 537 °C, detected in the H_2-TPR profile of V_2O_5-CeO_2-TiO_2 can be related to the reduction of surface oxygen of cerium, vanadium and cerium species [45,70-71]. For the V_2O_5-WO_3-TiO_2 sample, the peaks observed in the 400-600 °C temperature range and at 770 °C can be correlated with the reduction of vanadium [42,46] and tungsten [42,46,70] species, respectively. The V_2O_5-CeO_2-WO_3-TiO_2 sample displays similar (but less intensive) H_2 consumption peaks compared

to those obtained in the case of V_2O_5-WO_3-TiO_2 solid. This indicates the presence of reducible O, V, Ce and W species at the V_2O_5-WO_3-CeO_2-TiO_2 surface. Nevertheless, the reduction of tungsten species occurred at higher temperature in the presence of cerium (at 860 °C for VWCeTi and 770 °C for VWTi). This could confirm, in line with the NH_3-TPD results, the existence of strong interactions between the supported elements which affect the reducibility of catalysts.

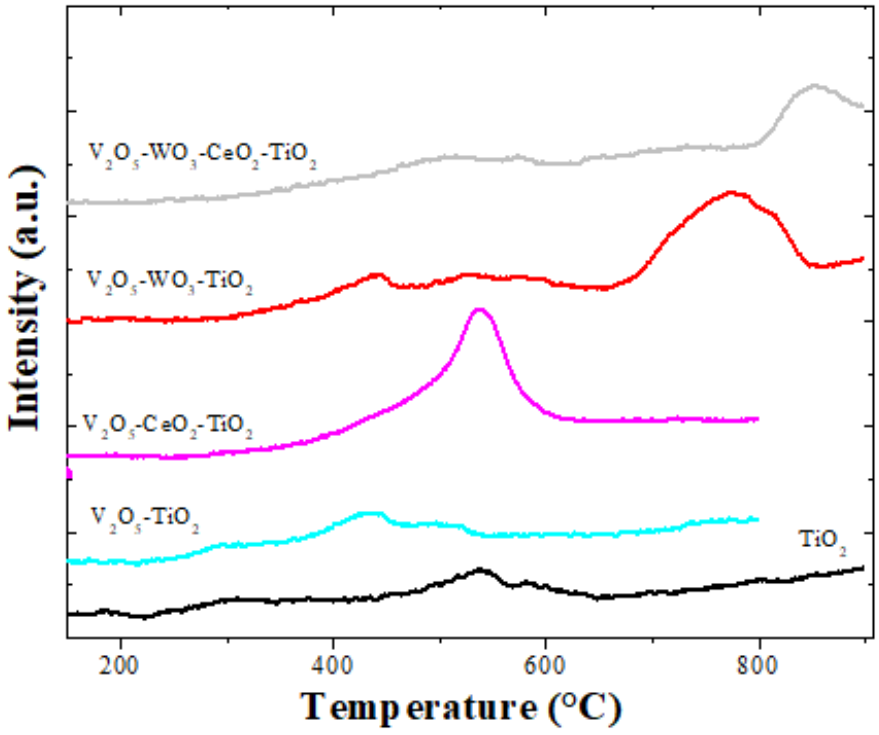

Figure 5. H_2-TPR profiles of aerogel catalysts.

3. 1. NO-SCR activity of aerogel catalysts

The NO conversion versus reaction temperature recorded for the aerogel catalysts are displayed in Fig 6. As it can be noticed, the V_2O_5-TiO_2 catalyst is more active than TiO_2 support for the NO reduction, particularly between 200 and 400 °C. This is due to the presence of active redox sites generated by vanadium species at the catalyst surface, which improves the SCR activity of solid, especially below 400 °C [46]. Nevertheless, only a

maximum of ~ 67 % NO conversion into N_2 is obtained over the V_2O_5-TiO_2 catalyst at 450 °C. The addition of tungsten into V_2O_5-TiO_2 sample decreases the SCR activity between 200 and 410 °C but it increases the NO conversion (~ 68 %) into N_2 at high temperatures (T > 420 °C). The enhancement of the SCR activity of the V_2O_5-WO_3-TiO_2 sample at high temperature can be correlated with the reactivity of acidic sites created by tungsten species. In fact, it was reported that tungsten oxide acts as a promoter owing to its Brønsted acidity which enhances ammonia adsorption on the catalyst during the SCR reaction [34]. The V_2O_5-CeO_2-TiO_2 solid demonstrates much higher SCR activity than those obtained over V_2O_5-TiO_2 and V_2O_5-WO_3-TiO_2. It exhibits, thanks to the redox sites created by cerium species, more than 80 % NO conversion into N_2 between 320 and 410 °C. This underlines, in agreement with our previous study [45], the crucial role of the OSC and redox performance of cerium species for DeNOxing at low temperature. Markedly, the DeNOx activity of V_2O_5-WO_3-CeO_2-TiO_2 catalyst is clearly higher than those obtained over all the other samples, in the whole temperature range of the experiment (150-500 °C). Hence, the T 50 and T 90 (temperatures for which 50 % and 90 % of NO conversions into N_2 are achieved) are: 245 and 320 °C, respectively. Taking into account the characterization results, demonstrating that V_2O_5-WO_3-CeO_2-TiO_2 develops the lowest surface area and acidity, it can be suggested, in line with the result already obtained by Hu et al. [44] for comparable systems (CeO_2-V_2O_5-WO_3/TiO_2) that, in this case, the BET surface area is not responsible for the catalytic activity. Therefore, the superior SCR performance of the new V_2O_5-WO_3-CeO_2-TiO_2 catalyst can be essentially related to a good mobility of surface oxygen species and a high reactivity of surface acid and redox sites, most probably due to the existence of strong interactions between the supported actives elements, mainly Ce↔V and Ce↔W. It should be also mentioned that the decrease of the NO conversion at high temperature for all the samples, except for V_2O_5-WO_3-TiO_2 solid, can be explained by the absence of active acidic sites for high temperature at their surfaces. In

fact, it was reported that the surface acidity of catalyst plays an important role in the adsorption and activation of ammonia, especially at high temperature [72].

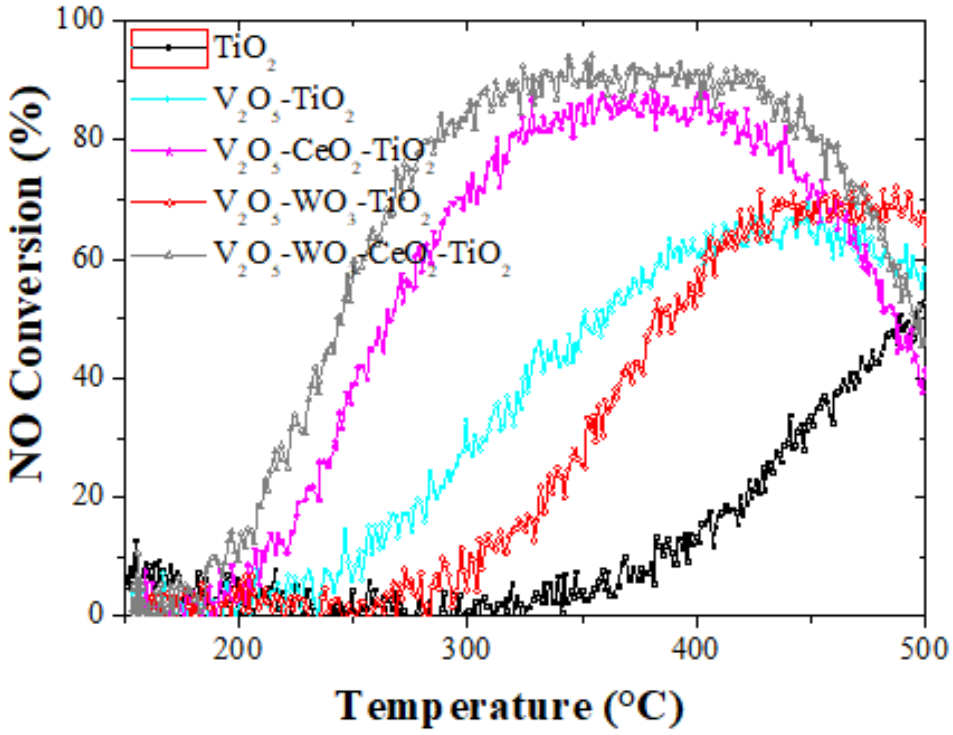

Figure 6. NO conversion versus reaction temperature over the aerogel catalysts.

4. Conclusion

In this study, new W and/or Ce modified V_2O_5-TiO_2 aerogel catalysts (V_2O_5-TiO_2, V_2O_5-WO_3-TiO_2, V_2O_5-CeO_2-TiO_2 and V_2O_5-WO_3-CeO_2-TiO_2) were prepared, characterized and tested in the DeNOx process. The results show that the addition of WO_3 improves the surface acidity and, consequently, the high temperature SCR-activity of V_2O_5-TiO_2 derived sol gel catalyst. However, the presence of CeO_2 enhances the redox performance of the later catalyst and obviously increases its SCR activity at low temperature. Among all the samples investigated, the new aerogel V_2O_5-WO_3-CeO_2-TiO_2, which exhibits the lowest surface area and acidity, was found to be the most active catalyst for the NO removal with 60 % and above 90 % of NO conversions into N_2 at 250 °C and in the 320-420 °C temperature range,

respectively. The highest SCR activity of this novel aerogel system was correlated with a high reactivity of surface acid and redox sites, most probably induced by the strong interactions developed between the supported actives elements, mainly Ce↔V and Ce↔W.

Acknowledgements

The authors wish to express their sincere thanks to Thomas Cacciaguerra for XRD analysis. The Franco-Tunisian Cooperation (French Institute of Tunisia, SSHN grant) and Laboratory of Chemistry of Materials and Catalysis (LCMC) of Tunisia are gratefully acknowledged for the Financial support.

References

[1] Y. Slimanin, A. Selmi, E. Hannachi, M. A. Almessiere1, M. Mumtaz, A. Baykal, I. Ercan, Study of tungsten oxide efect on the performance of $BaTiO_3$ ceramics, J. Mater. Sci.: Mater. Electron. 30 (14) (2019) 13509-13518.

[2] Y. Slimani, B. Unal, E. Hannachi, A. Selmid, M.A. Almessiere, M. Nawaz , A. Baykal , I. Ercan, M. Yildiz, Frequency and dc bias voltage dependent dielectric properties and electrical conductivity of $BaTiO_3$eSrTiO_3/(SiO_2)x nanocomposites Ceram. Int. 45 (2019) 11989-12000.

[3] M. H. A. Mhareb, Y. Slimani, Y. S. Alajeramid, M. I. Sayyed, E. Lacomme, M. A. Almessiere, Structural and radiation shielding properties of $BaTiO_3$ ceramic with different concentrations of Bismuth and Ytterbium Ceram. Int. 46 (18) (2020) 28877-28886.

[4] M. A. Almessiere, Y. Slimani, S. Güner , M. Nawaz, A. Baykal, F. Aldakheel, S. Akhtar, I. Ercan, İ. Belenli, B. Ozçelik, Magnetic and structural characterization of Nb^{3+}-substituted $CoFe_2O_4$ nanoparticles, Ceram. Int. 45 (2019) 8222-8232.

[5] E. Hannachi, Y Slimani, M. K. Ben Salem, A. Hamrita, A. L. Al-Otaibi, M. A. Almessiere, M. Ben Salem, F ; Ben Azzouz,Fluctuation induced conductivity studies in

$YBa_2Cu_3O_y$ compound embedded by superconducting nano-particles Y-deficient $YBa_2Cu_3O_y$: effect of silver inclusion, Indian J. Phys. 90 (2016) 1009-1018.

[6] Y. Slimani, E. Hannachi, F. Ben Azzouz, M. Ben Salem, Impact of planetary ball milling parameters on the microstructure and pinning properties of polycrystalline superconductor $Y_3Ba_5Cu_8O_y$, Cryogenics 92 (2018) 5-12.

[7] M. A. Almessiere, Y. Slimani, H. S. El Sayed, A. Baykal, Morphology and magnetic traits of strontium nanohexaferrites: Effects of manganese/yttrium co-substitution J. Rare Earths 37(7) (2019) 732-740.

[8] E. Hannachi, Y. Slimani, F. Ben Azzouz, A. Ekicibil, Higher intra-granular and inter-granular performances of YBCO superconductor with TiO2 nano-sized particles addition Ceram. Int. 44 (2018) 18836-18843.

[9] Y. Slimani, E. Hannachi, A. Hamrita, M.K. Ben Salem, F. Ben Azzouz, A. Manikandan, M. Ben Salem, Comparative investigation of the ball milling role against hand grinding on microstructure, transport and pinning properties of $Y_3Ba_5Cu_8O_{18\pm\delta}$ and $YBa_2Cu_3O_{7-\delta}$, Ceram. Int. 44 (2018) 19950-19957.

[10] Y. Slimani, A. Selmi, E. Hannachi, M. A. Almessiere, A. Baykal, I. Ercan, Impact of ZnO addition on structural, morphological, optical, dielectric and electrical performances of $BaTiO_3$ ceramics, J. Mater. Sci.: Mater. Electron. 30 (2019) 9520-9530.

[11] A. D. Korkmaz, S. Guner, Y. Slimani, H. Gungunes, Md. Amir, A. Manikandan, A. Baykal, Microstructural, Optical, and Magnetic Properties of Vanadium-Substituted Nickel Spinel Nanoferrites J. Supercond. Nov. Magn. 32(4) (2019) 1057-1065.

[12] M. R. Koblischka, A. Koblischka-Veneva, X. L. Zeng, E. Hannachi,Y. Slimani, Microstructure and Fluctuation-Induced Conductivity Analysis of Bi2Sr2CaCu2O8+δ (Bi-2212) Nanowire Fabrics, Crystals 10 (11) (2020) 986.

[13] S. Akhtar, S. Rehman, M. A. Almessiere, F. A. Khan, Y. Slimani, A. Baykal,Synthesis of $Mn_{0.5}Zn_{0.5}Sm_xEu_xFe_{1.8-2x}O_4$, Nanoparticles via the Hydrothermal Approach Induced Anti-Cancer and Anti-Bacterial Activities, Nanomaterials 9 (2019) 1635.

[14] E. W. McFarland, H. Metiu, Catalysis by Doped Oxides, Chem. Rev. 113 (2013) 4391–4427.

[15] D. Damma, P. R. Ettireddy, B. M. Reddy, P. G. Smirniotis, A Review of Low Temperature NH_3-SCR for Removal of NO_x, Catalysts 9 (2019) 349.

[16] Gao F, Tang X, Yi H, Zhao S, Li C, Li J, Shi Y, Meng X, A Review on Selective Catalytic Reduction of NOx by NH_3 over Mn-Based Catalysts at Low Temperatures: Catalysts, Mechanisms, Kinetics and DFT Calculations. Catalysts 7 (2017) 199-231.

[17] Xie W, Zhang G, Mu B, Tanga Z, Zhang J, The promoting effect of palygorskite on CeO_2-WO_3-TiO_2 catalyst for the selective catalytic reduction of NOx with NH_3, Appl. Clay Sci. 192 (2020) 105641.

[18] Busca G, Lietti L, Ramis G, Berti F, Chemical and mechanistic aspects of the selective catalytic reduction of NOx by ammonia over oxide catalysts: a review. Appl. Catal. B 18 (1998) 1–36.

[19] Fan X, Kang S, Li J, Plasma-enhanced hydrolysis of urea and SCR of NOx over V_2O_5-MoO_3/TiO_2: Decrease of reaction temperature and increase of NOx conversion, Fuel 277 (2020) 118155.

[20] Jiang Y, Lu M, Liu S, Bao C, Liang G, Lai C, Shia W, Ma S, Deactivation by HCl of CeO_2–MoO_3/TiO_2 catalyst for selective catalytic reduction of NO with NH_3, RSC Adv. 8 (2018) 17677-16684.

[21] Chen, C., Cao, Y., Liu, S., Chen, J., Jia, W.,. Review on the latest developments in modified vanadium- titanium- based SCR catalysts. Chinese J. Catal. 39 (2018) 1347–1365.

[22] Shan W, Song H, Catalysts for the selective catalytic reduction of NOx with NH_3 at low temperature Catal. Sci. Technol. 5 (2015) 4280.

[23] Xue H, Li G, Liu P, Wang F, Bai Y, Wang K, Review of Catalysts for Selective Catalytic Reduction(SCR) of NOx, Advanced Materials Research Vols. 550-553 (2012) 119-123.

[24] Lai J K, Wachs I E, A Perspective on the Selective Catalytic Reduction (SCR) of NO with NH_3 by Supported V_2O_5 -WO_3 /TiO_2 Catalysts, ACS Catal. 8 (2018) 6537–6551.

[25] Lian Z, Li Y, Shan W, He H, Recent Progress on Improving Low-Temperature Activity of Vanadia-Based Catalysts for the Selective Catalytic Reduction of NOx with Ammonia. Catalysts, 10 (2020) 1421.

[26] Marberger A, Elsener M, Ferri D, Kröcher O, VOx Surface Coverage Optimization of V_2O_5/WO_3-TiO_2 SCR Catalysts by Variation of the V Loading and by Aging, Catalysts 5 (2015) 1704-1720.

[27] Qi C, Bao W, Wang L, Li H, Wu W, Study of the V_2O_5–WO_3/TiO_2 Catalyst Synthesized from Waste Catalyst on Selective Catalytic Reduction of NOx by NH_3. Catalysts 7 (2017) 110.

[28] Shang X, Hu G, He C, Zhao J, Zhang F, Xu Y, Zhang Y, Li J, Chen J, Regeneration of full-scale commercial honeycomb monolith catalyst (V_2O_5–WO_3/TiO_2) used in coal-fired power plant. J. Ind. Eng. Chem. 18 (2012) 513–519.

[29] Zhang W, Qi S, Pantaleo G, Liotta L F, WO_3–V_2O_5 Active Oxides for NOx SCR by NH_3: Preparation Methods, Catalysts Composition, and Deactivation Mechanism. A Review Catalysts, 9 (2019) 527.

[30] Fountzoula Ch, Spanos N, Matralis H K, Kordulis Ch, Molybdenum-titanium oxide catalysts: the influence of the preparation conditions for the selective catalytic reduction of NO by NH_3. Appl. Catal . B Environm. 35, (2002) 295-304.

[31] Han L, Cai S, Gao M, Hasegawa J Y, Wang P, Zhang J, Shi L, Zhang D, Selective Catalytic Reduction of NO_x with NH_3 by Using Novel Catalysts: State of the Art and Future Prospects. *Chem. Rev.* 119, 19 (2019) 10916–10976

[32] Yu W, Wu X, Si Z, Weng D, Influences of impregnation procedure on the SCR activity and alkali resistance of V_2O_5-WO_3/TiO_2 catalyst. Appl. Surf. Sci. 283 (2013) 209–214.

[33] Dong G J, Zhang Y F, Yuan Z, Yang B, Effect of the pH value of precursor solution on the catalytic performance of V_2O_5 -WO_3 /TiO_2 in the low temperature NH_3-SCR of NOx. J. Fuel Chem. Technol. 42 (2014) 1455–1463.

[34] He Y, Ford M E, Zhu M, Liu Q, Tumuluri, U, Wu Z, Wachs I E, Influence of catalyst synthesis method on selective catalytic reduction (SCR) of NO by NH_3 with V_2O_5-WO_3/TiO_2 catalysts, Appl. Catal. B Environm. 193 (2016) 141–150**.**

[35] Pang L, Fan C, Shao L, Yi J, Cai X, Wang J, Kang M, Li T, Effect of V_2O_5/WO_3- TiO_2 catalyst preparation method on NOx removal from diesel exhaust. Chinese J. Catal. 35 (2014) 2020–2028.

[36] Meiqing S, Lili X, Jianqiang W, Chenxu L, Wulin W, Jun W, Yanping Z, Effect of Synthesis Methods on Activity of V_2O_5/CeO_2/WO_3-TiO_2 Catalyst for Selective Catalytic Reduction of NOx with NH_3. J. Rare Earths 34 (2016) 259–267.

[37] Reiche M, Buergi T, Baiker A, Scholz A, Schnyder B, Wokaun A, Vanadia and Tungsta Grafted on TiO_2 : Influence of the Grafting Sequence on Structural and Chemical Properties. Appl. Catal. A 198 (2000) 155–169.

[38] Chen L, Li J H, Ge M F, Zhu R, Enhanced activity of tungsten modified CeO_2/TiO_2 for selective catalytic reduction of NOx with ammonia, Catalysis Today 153 (2010) 77–83.

[39] Huang Y, Tong Z Q, Wu B, Zhang J F, Low temperature selective catalytic reduction of NO by ammonia over V_2O_5–CeO_2/TiO_2, J. Fuel Chem. Technol. 36 (2008) 616–620.

[40] Shan W, Geng Y, Zhang Y, Lian Z, He H, A CeO_2/ZrO_2-TiO_2 Catalyst for the Selective Catalytic Reduction of NOx with NH_3. Catalysts 8 (2018) 592

[41] Qi G, Yang R T, Chang R, MnOx–CeO_2 mixed oxides prepared by co-precipitation for selective catalytic reduction of NO with NH_3 at low temperatures, Appl. Catal. B Environm. 51 (2004) 93–106.

[42] Chen L, Li J H, Ge M F, Promotional effect of Ce-doped V_2O_5-WO_3/TiO_2 with low vanadium loadings for selective catalytic reduction of NOx by NH_3, J. Phys. Chem. C 113 (2009) 21177–21184.

[43] Cheng K, Liu J, Zhang T, Li J, Zhao Z, Wei Y, Jiang G, Duan A, Effect of Ce doping of TiO_2 support on NH_3-SCR activity over V_2O_5–WO_3/CeO_2–TiO_2 catalyst. J. Environ. Sci. 26 (2014) 2106-2113.

[44] Hu G, Yang J, Tian Y, Kong B, Liu Q, Ren S, Li J, Kong M, Effect of Ce doping on the resistance of Na over V_2O_5-WO_3/TiO_2 SCR catalysts. Mater. Res. Bull. 104 (2018) 112–118.

[45] Arfaoui J, Ghorbel A, Petitto C, Delahay G, Novel V_2O_5-CeO_2-TiO_2-SO_4^{2-} nanostructured aerogel catalyst for the low temperature selective catalytic reduction of NO by NH_3 in excess O_2, Appl. Catal. B: Environm. 224, (2018) 264-275.

[46] Arfaoui J, Ghorbel A, Petitto C, Delahay G, A new V_2O_5-MoO_3-TiO_2-SO_4^{2-} nanostructured aerogel catalyst for Diesel DeNOx technology. New J. Chem. 44, (2020) 16119-16134.

[47] Arfaoui J, Ghorbel A, Petitto C, Delahay G, New MoO_3-CeO_2-ZrO_2 and WO_3-CeO_2-ZrO_2 nanostructured mesoporous aerogel catalysts for the NH_3-SCR of NO from diesel engine exhaust. J. Ind. Eng. Chem. 95, (2021) 182-189.

[48] Arfaoui J, Ghorbel A, Petitto C, Delahay G, New Mn-TiO_2 aerogel catalysts for the low temperature Selective Catalytic Reduction of NOx, J. Sol-Gel Sci. Technol. 97 (2021) 302–310.

[49] P. Forzatti, Present status and perspectives in de-NOx SCR catalysis. Appl. Catal. A General, 221-236, 222 (2001)

[50] W. Gao, Z. Zhang, J. Li, Y. Ma, Y. Qu, Surface engineering on CeO_2 nanorods by chemical redox etching and their enhanced catalytic activity for CO oxidation. Nanoscale 11686–11691, 7 (2015)

[51] H. Jensen, A. Soloviev, Z. Li, E. G. Søgaard, XPS and FTIR investigation of the surface properties of different prepared titania nano-powders. Appl. Surf. Sci. 239–249, 246 (2005)

[52] Y. Iida, S. Ozak, Grain Growth and Phase Transformation of Titanium Oxide During Calcination, J. Am. Ceram. Soc. 120-127, 44 (1961)

[53] K.-N. P. Kumar, Growth of rutile crystallites during the initial stage of anatase to rutile transformation in pure titania and in titanis alumina nanocomposites, Scr. Metall. Mater.32 (1995) 873-877.

[54] Thommes M, Kaneko K, Neimark A V, Olivier J P, Rodriguez-Reinoso F, Rouquerol J, Sing K S W, Physisorption of gases, with special reference to the evaluation of surface area and pore size distribution (IUPAC Technical Report), Pure Appl. Chem. 87 (2015) 1051–1069.

[55] López-Mendoza M A, Nava R, Peza-Ledesma C, Millán-Malo B, Huirache-Acuña R, Skewes P, Rivera-Muñoz E M, Characterization and catalytic performance of Co-Mo-W sulfide catalysts supported on SBA-15 and SBA-16 mechanically mixed, Catal. Today 271 (2016) 114-126.

[56] Imran G, Maheswari R, Mn-incorporated SBA-1 cubic mesoporous silicates: Synthesis and characterization. Mater. Chem. Phys. 161 (2015) 237-242.

[57] Segura Y, Chmielarz L, Kustrowski P, Cool P, Dziembaj R, Vansant E F, Characterisation and reactivity of vanadia–titania supported SBA-15 in the SCR of NO with ammonia, Appl. Catal. B: Environ. 61 (2005) 69–78.

[58] Morey M, Davidson A, Eckert H, Stucky G, Pseudotetrahedral O3/2V = O centers immobilized on the walls of a mesoporous, cubic MCM-48 support: preparation, characterization, and reactivity toward water As investigated by 51V NMR and UV–vis spectroscopies, Chem. Mater. 8 (1996) 486–492.

[59] Shao Y, Wang L, Zhang J, Anpo M, Synthesis of hydrothermally stable and longrange ordered Ce-MCM-48 and Fe-MCM-48 materials, J. Phys. Chem. B 109 (2005) 20835–20841.

[60] Keller D E, Visser T, Soulimani F, Koningsberger D C, Weckhuysen B M, Hydration effects on the molecular structure of silica-supported vanadium oxide catalysts: a combined IR, Raman, UV–vis and EXAFS study, Vib. Spectrosc. 43 (2007) 140–151.

[61] Yang X L, Dai W L, Gao R, Chen H, Li H, Cao Y, Fan K, Synthesis, characterization and catalytic application of mesoporous W-MCM-48 for the selective oxidation of cyclopentene to glutaraldehyde, J. Mol. Catal A : Chem. 241 (2005) 205-214.

[62] Murgia V, Torres E M F, Gottifredi J C, Sham E L, Sol-gel synthesis of V_2O_5–SiO_2 catalyst in the oxidative dehydrogenation of n-butane. Appl. Catal. A 312 (2006) 134–143.

[63] Roth W J, Gil B, Makowski W, Sławek A, Korzeniowska A, Grzybek J, Siwek M, Michorczyk P, Framework-substituted cerium MCM-22 zeolite and its interlayer expanded derivative MWW-IEZ, Catal. Sci. Technol. 6 (2016) 2742-2753.

[64] Wu Y, Wang J, Liu P, Zhang W, Gu J, Wang X, Framework-substituted lanthanide MCM-22 zeolite: synthesis and characterization, J. Am. Chem. Soc. 132 (2010) 17989–17991.

[65] Song Z, Xing Y, Zhang T, Zhao J, Wang J, Mao Y, Zhao B, Zhang X, Zhao M, Ma Z, Effectively promoted catalytic activity by adjusting calcination temperature of Ce-Fe-Ox catalyst for NH_3-SCR, Appl Organometal Chem. e5446. (2019) https://doi.org/10.1002/aoc.5446.

[66] Cha W, Ehrman S H, Jurng J, CeO_2 added V_2O_5/TiO_2 catalyst prepared by chemical vapor condensation (CVC) and impregnation method for enhanced NH_3-SCR of NOx at low temperature, J. Environ. Chem. Eng. 4 (2016) 556-563.

[67] Gannoun C, Delaigle R, Eloy P, Debecker D P, Ghorbel A, Gaigneaux E M, Effect of support on V_2O_5 catalytic activity in chlorobenzene oxidation, Appl. Catal., A, 447–448 (2012) 1–6.

[68] Sun C, Dong L, Yu W, Liu L, Li H, Gao F, Dong L, Chen Y, Promotion effect of tungsten oxide on SCR of NO with NH_3 for the V_2O_5-$WO_3/Ti_{0.5}Sn_{0.5}O_2$ catalyst: Experiments combined with DFT calculations. J. Mol. Catal. A Chem. 346 (2011) 29–38.

[69] Zhang S, Li H, Zhong Q, Promotional Effect of F-Doped V_2O_5 -WO_3/TiO_2 Catalyst for NH_3 -SCR of NO at Low-Temperature. Appl. Catal. A 435 (2012) 156-162.

[70] Chen L, Weng D, Wang J, Weng D, Cao L, Low- temperature activity and mechanism of WO_3- modified CeO_2- TiO_2 catalyst under NH_3- NO/NO_2 SCR conditions, Chinese J. Catal. 39, (2018) 1804-1813.

[71] Liu, Z, Zhang, S, Li J, Zhu J Ma, L, Novel V_2O_5-CeO_2/TiO_2 catalyst with low vanadium loading for the selective catalytic reduction of NOx by NH_3, Appl. Catal. B: Environ. 11-19 (2014) 158-159.

[72] Forzatti P, Present status and perspectives in de-NOx SCR catalysis. Appl. Catal. A 222 (2001) 221-236.